LETTER **Communicated by Kunal Garg**

Fixed-Time Stable Neurodynamic Flow to Sparse Signal Recovery via Nonconvex $L_{1-\beta 2}$-Norm

You Zhao
Zhaoyou1991sdtz@163.com
Key Laboratory of Dependable Services Computing in Cyber Physical Society-Ministry of Education, College of Computer Science, Chongqing University, Chongqing 400044, China

Xiaofeng Liao
xfliao@cqu.edu.cn
IEEE Fellow, and Key Laboratory of Dependable Services Computing in Cyber Physical Society-Ministry of Education, College of Computer Science, Chongqing University, Chongqing 400044, China

Xing He
hexingdoc@swu.edu.cn
Chongqing Key Laboratory of Nonlinear Circuits and Intelligent Information Processing, College of Electronics and Information Engineering, Southwest University, Chongqing 400715, China

This letter develops a novel fixed-time stable neurodynamic flow (FTSNF) implemented in a dynamical system for solving the nonconvex, nonsmooth model $L_{1-\beta 2}$, $\beta \in [0, 1]$ to recover a sparse signal. FTSNF is composed of many neuron-like elements running in parallel. It is very efficient and has provable fixed-time convergence. First, a closed-form solution of the proximal operator to model $L_{1-\beta 2}$, $\beta \in [0, 1]$ is presented based on the classic soft thresholding of the L_1-norm. Next, the proposed FTSNF is proven to have a fixed-time convergence property without additional assumptions on the convexity and strong monotonicity of the objective functions. In addition, we show that FTSNF can be transformed into other proximal neurodynamic flows that have exponential and finite-time convergence properties. The simulation results of sparse signal recovery verify the effectiveness and superiority of the proposed FTSNF.

1 Introduction

Thanks to the pioneering work of Candès, Romberg, and Tao (2006), compressed sensing (CS) has emerged as a promising method for restoring the

Xiaofeng Liao is the corresponding author.

Neural Computation **34, 1727–1755** (2022)
https://doi.org/10.1162/neco_a_01508
© 2022 Massachusetts Institute of Technology

Downloaded from http://direct.mit.edu/neco/article-pdf/34/8/1727/2034959/neco_a_01508.pdf by HONG KONG POLYTECHNIC UNIVERSITY user on 13 August 2024

usefulness of sparse signals with respect to a given sensing matrix and observed signal. Given this, three important typical problems must be addressed. The first is how to build a sparse signal recovery model so that its optimal solution is close to the sparsest signal, such as minimization models with the L_1-norm, L_0-norm, L_p-norm, and L_{1-2} hybrid norm. The second is to study different types of optimization methods that are capable of recovering sparse signals (called sparse signal recovery or sparse signal reconstruction). The third is to construct sensing matrices to analyze the sparse recovery models and test the performance characteristics of correlated sparse optimization methods. It is worth noting that sparse signal recovery plays an important role in CS. Moreover, it is the bridge that establishes the connection between the first and the third problems in CS. This motivates us to focus the research in this letter on sparse signal recovery.

Sparse signal recovery, as a fundamental theory of CS, has been intensively investigated in recent years as it requires a remarkably lower sampling than that of Nyquist. It has been widely applied in image processing (Bach, Mairal, Ponce, & Sapiro, 2010), data analysis (Huang & Aviyente, 2006), pattern recognition (Wright, Ma, Mairal, Sapiro, Huang, & Yan, 2010), medical imaging processing (Chen et al., 2014), and smart grids (Li, Yu, Yu, Chen, & Wang, 2016). The purpose of sparse signal recovery is to find a parsimonious feature of the signal by making use of a few elements of an overcomplete dictionary,

$$\mathrm{b} = Ax + e,$$

where $\mathrm{b} \in R^n$ is the observed value corrupted by noise $e \in R^n$, $x \in R^n$ is a sparse signal with s-sparsity, and $A \in R^{m\times n}(m \ll n)$ is the measurement matrix (i.e., dictionary). This is generally ill posed and difficult to restore x from the compressed measurement b due to $m \ll n$. Candès (2008) has shown that x can be faithfully recovered with the upper bound of error, which is determined by the noise intensities, provided that the measurement matrix A fulfills some stable embedding conditions.

The problem of sparse signal recovery can be cast as

$$\min_{x\in R^n} \ \lambda\|x\|_0 + \frac{1}{2}\|Ax - \mathrm{b}\|_2^2,$$

where $\|\cdot\|_0$ is L_0-norm, which indicates the number of nonzero elements in the vector x. $\lambda > 0$ is a trade-off parameter. Unfortunately, it is NP-hard to obtain the global optimal solution of the L_0-norm minimization problem. According to the restricted isometry property (RIP) condition, one can equivalently adopt the L_1-norm for replacement L_0-norm with a high probability of evaluating the expected sparse signal x by addressing the following L_1-norm minimization problem,

$$\min_{x\in R^n} \ \lambda\|x\|_1 + \frac{1}{2}\|Ax - \mathrm{b}\|_2^2, \tag{1.1}$$

Downloaded from http://direct.mit.edu/neco/article-pdf/34/8/1727/2034959/neco_a_01508.pdf by HONG KONG POLYTECHNIC UNIVERSITY user on 13 August 2024

where $\|x\|_1 = \sum_{i=1}^{n} |x_i|$. The L_1-norm minimization problem 1 is easier to handle as it is convex. Problem 1 is therefore widely used in sparse signal recovery such as blind source separation (Li, Cichocki, & Amari, 2006), variable selection (Fan & Li, 2001), and face recognition (Wagner et al., 2011). Some numerical iterative algorithms are available for solving the L_1-norm minimization problem, for example, basis pursuit (BP) (Candès et al., 2006) and the augmented Lagrangian method (Afonso, Bioucas-Dias, & Figueiredo, 2010; Tomioka & Sugiyama, 2009).

Recently, there has been an increasing number of applications for nonconvex measurements as alternatives to the convex L_1-norm. In particular, the application of the nonconvex L_p, $p \in (0, 1)$-norm (quasi-norm) in Chartrand (2007) and Zuo, Meng, Zhang, Feng, and Zhang (2013) can be seen as a continuation strategy for approximating the L_0-norm in terms of $p \to 0$. To address the p-norm minimization problem, optimization strategies including iterative reweighting approaches (Lai, Xu, & Yin, 2013) and half-thresholding algorithms (Xu, Chang, Xu, & Zhang, 2012; Wu, Sun, & Li, 2016) have been studied. Other nonconvex variants of the L_1-norm have been investigated, such as transforming the L_1-norm (Zhang & Xin, 2018) and capping the L_1-norm (Lou, Yin, & Xin, 2016). Recently, hybrid norm models such as the difference of L_1-norm and L_2-norm (L_{1-2}) (Yin, Lou, He, & Xin, 2015; Lou & Yan, 2018), the difference of L_1-norm and L_p-norm (L_{1-p}) (Wang & Zhang, 2017), and the difference of L_p-norm and L_q-norm (L_{p-q}) (Zhao, He, Huang, & Huang, 2018) have been studied for recovering sparse signals.

Neurodynamic approaches have received increasing attention because they can efficiently solve optimization problems by hardware analog circuits in parallel. Liu and Wang (2008) designed a one-layer recurrent neural network to address linear programming based on a discontinuous activation function. Later, Liu, Cao, and Chen (2010) proposed a novel neural network approach to deal with linear programming with a finite-time stability. Liu, Zeng, and Wang (2017) investigated the multistability of delayed recurrent neural networks with the Mexican hat activation function. Garg and Panagou (2021) proposed several fixed-time stable gradient flows. In addition, some distributed neurodynamic flows with fixed-time or predefined-time convergence rates for distributed optimization and resource allocation were studied in Li, Yu, Zhou, and Ren (2017), Lin, Wang, Li, and Yu (2020), and Garg and Baranwal (2020). Rozell, Johnson, Baraniuk, and Olshausen (2008) first proposed a continuous-time local competitive algorithm (LCA) approach for sparse coding based on thresholding functions. Balavoine, Rozell, and Romberg (2013) proved that the local competitive algorithm (LCA) has an exponential convergence rate. Li, Wang, and Kwong (2020) investigated a discrete-time neurodynamic approach to deal with a nonnegative matrix factorization problem with sparsity constraints. Liu and Wang (2016) and Xu, Liu, and Huang (2019) proposed several continuous/discrete-time projection neural networks for

Downloaded from http://direct.mit.edu/neco/article-pdf/34/8/1727/2034959/neco_a_01508.pdf by HONG KONG POLYTECHNIC UNIVERSITY user on 13 August 2024

the L_1-norm minimization problem on the strength of projection operators. Feng, Leung, Constantinides, and Zeng (2017) adopted a modified Lagrangian neural network based on a locally competitive algorithm (BP-LPNN) to solve problem 1 to obtain sparse signals with and without noise measurement. By smoothing approximation techniques, Bian and Chen (2012) developed a smoothing projection neural network, and Zhao, Liao, He, Tang, and Deng (2021) proposed a smoothing inertial neurodynamic approach by introducing an inertial term to address the nonconvex L_p-norm minimization problem. To tackle the nonconvex hybrid norm models, Zhu, Wang, He, and Zhao (2018) investigated an inertial neural network based on projection operators (IPNN) for solving the L_{1-2} hybrid norm minimization problem. Wang and Zhang (2017) investigated a smoothing projection neural network (SPNN) to address a generalized L_{1-p}, $(2 > p > 1)$ optimization problem to recover sparse signals. Later, Zhao et al. (2018) studied a more generalized hybrid norm model, the L_{p-q} hybrid norm model, for recovering sparse signals accurately with noise-free measurements. However, the neurodynamic flows already noted are still unclear with regard to convergence rates (Zhao, He, Huang, & Huang, 2018; Liu & Wang, 2016) or only exponential convergence rates (Balavoine et al., 2013). This cannot ensure the convergence of sparse recovery when the signal changes very quickly or the speed of the signal recovery response is urgently needed. Two dynamical systems with finite-time and fixed-time convergence were proposed to solve the L_1-norm minimization problem with noise measurement in Yu, Zheng, and Barbot (2017) and Ren et al. (2019). Two neurodynamic flows for solving the L_1-norm minimization problem to achieve a sparse signal with finite-time and fixed-time convergence rates under noise-free measurement were proposed by He and his collaborators (Wen, Wang, & He, 2020; He, Wen, & Huang, 2021). Garg and Baranwal (2020) proposed a continuous-time accelerated algorithm (CAPPA) based on the proximal operator of the L_1-norm and sliding mode technique. CAPPA got a fixed-time convergence rate to seek a sparse signal by minimizing the L_1-norm with noise measurement.

Hybrid norm models are a type of sparse recovery model that have at least two kinds of norms. Research on such models and their related methods is becoming increasingly important in computer science, among which the unconstrained L_{1-2} model is the most popular. Recently, the L_{1-2} sparse model has been applied to signal processing and compressed sensing, has derived meaningful and favorable results (Yin, Lou, He, & Xin, 2015; Lou & Yan, 2018), and has even outperformed the L_1- and L_p-norms in promoting sparsity under some conditions. Numerical experiments demonstrated that the L_{1-2} model is a valuable sparse recovery model to a certain extent. To the best of our knowledge, only three studies—by Zhu et al. (2018), Wang and Zhang (2017), and Zhao et al. (2018)—have been provided, applying neurodynamic flows to solve related problems. However, they only gave the convergence analysis of their neurodynamic flows and did not involve

Downloaded from http://direct.mit.edu/neco/article-pdf/34/8/1727/2034959/neco_a_01508.pdf by HONG KONG POLYTECHNIC UNIVERSITY user on 13 August 2024

their convergence rates. Whether faster neurodynamic flows exist with a fixed-time convergence rate to solve the $L_{1-\beta 2}, \beta \in (0, 1]$ problem motivates us to investigate this problem.

Based on the above discussion, we propose a novel neurodynamic flow approach with a fixed-time convergence rate for solving the nonconvex $L_{1-\beta 2}, \beta \in (0, 1]$ and convex $L_{1-\beta 2}, \beta = 0$ problems with noise measurement:

$$\min_{x \in R^n} \lambda \left(\|x\|_1 - \beta \|x\|_2 \right) + \frac{1}{2} \|Ax - \mathrm{b}\|_2^2, \beta \in [0, 1]. \tag{1.2}$$

Note that problem (1.2) is nonconvex when $\beta \in (0, 1]$ and reduces to the classical Lasso problem if $\beta = 0$. Thus, the model with $L_{1-\beta 2}$ is a generalization model of Lasso and L_{1-2}.

The main contributions of this letter are as follows:

- A novel fixed-time stable neurodynamic flow (FTSNF) is proposed to solve the nonconvex $L_{1-\beta 2}$ (convex $L_{1-\beta 2}, \beta = 0$) minimization problem to recover sparse signals. To the best of our knowledge, this is the first attempt to design a neurodynamic flow to address this problem with a fixed-time convergence rate. Compared with the existing neurodynamic flows for the convex L_1-minimization problem with finite/fixed-time convergence rates (Yu et al., 2017; Ren et al., 2019; Wen, Wang, & He, 2020; Garg & Baranwal, 2020), our proposed FTSNF not only tackles the nonconvex equation 1.2 with $\beta \in (0, 1]$, but also solves convex L_1-minimization problems as a by-product. In addition, when $\beta = 0$, FTSNF reduces to the classical CAPPA (Garg & Baranwal, 2020).
- Since $L_{1-\beta 2}, \beta \in (0, 1]$ is nonconvex, the techniques in Yu et al. (2017), Ren et al. (2019), Wen et al. (2020), and Garg and Baranwal (2020) cannot be used directly for analyzing FTSNF. Thus, for analyzing our proposed FTSNF, we offer a new proof method that depends on the Lipschitz condition in theorems 1 and 2. This is different from Yu et al. (2017), Ren et al. (2019), Wen et al. (2020), and Garg and Baranwal (2020).
- A closed-form solution of the proximal operator to the $L_{\tau\lambda(1-\beta 2)}$ hybrid norm, $\tau, \lambda > 0, \beta \in [0, 1]$, is presented based on the classical soft thresholding of the L_1-norm. This is much more intuitive and concise than the proximal operator given in Lou and Yan (2018) and Liu and Pong (2017).
- By setting different parameters, the exponential, finite-time, and fixed-time convergence rates of FTSNF can also be achieved. This means that the proposed FTSNF has strong generalization ability.

The letter is arranged as follows. Definitions and lemmas are reviewed in section 2. In section 3, a closed-form solution of the proximal operator to $L_{1-\beta 2}, \beta \in [0, 1]$ is given. The new fixed-time stable neurodynamic flow

Downloaded from http://direct.mit.edu/neco/article-pdf/34/8/1727/2034959/neco_a_01508.pdf by HONG KONG POLYTECHNIC UNIVERSITY user on 13 August 2024

(FTSNF) is built, and its fixed-time convergence property is discussed. In section 4, some corollaries of the proposed FTSNF are provided. Several simulations on sparse signal recovery are displayed in section 5. Conclusions are presented in section 6.

Notations: Let $x^T y = \sum_{i=1}^{n} x_i y_i$. $\|x\|_2 = \left(\sum_{i=1}^{n} x_i^2\right)^{\frac{1}{2}}$ denotes the Euclidean norm. I is an identity matrix. $\mathbf{0} = (0, \ldots, 0)^T \in R^n, \mathbf{1} = (1, \ldots, 1)^T \in R^n$. diag $\{x\}$ represents the diagonal matrix constructed by the vector x. For $x \in R$, sign (x) is the signum function.

2 System Stability

Define a dynamic system as follows:

$$\dot{\vartheta}(t) = f(\vartheta(t)), \tag{2.1}$$

where $\vartheta(t) \in R^n$ is the system variable. Let ϑ^* be an equilibrium point of system 2.1, that is, it satisfies $f(\vartheta^*) = 0$.

System 2.1 has various convergence concepts—for example, Lyapunov stable around ϑ^*; globally asymptotically stable around ϑ^*; globally exponentially stable around ϑ^*; globally finite-time stable around ϑ^*; and globally fixed-time stable around ϑ^*, which are presented in the appendix.

Lemma 1 (Polyakov, 2012). *Let $V(x) : R^n \to R$ be a positive-definite, continuously differentiable function for system 2.1 that satisfies $\dot{V}(x) \leqslant -a_1 V(x)^{\alpha_1} - a_2 V(x)^{\alpha_2}$, where a_1, a_2, α_1, and α_2 are positive real numbers. For the different parameters of a_1, a_2, α_1, and α_1, $V(x)$ has the following finite time and fixed time convergence rate:*

1. *Time budget of finite-time convergence. If $a_1 > 0, a_2 = 0, 1 > \alpha_1 > 0$, then system 2.1 has a finite-time convergence property with a $T_{\max} \leqslant \frac{V(t_0)^{(1-\alpha_1)}}{a_1(1-\alpha_1)}$, which depends on the initial state $x(t_0)$.*
2. *Time budget of fixed-time convergence. If $a_1, a_2 > 0$, $1 > \alpha_1 > 0$, $\alpha_2 > 1$, system 2.1 achieves a fixed-time convergence with a $T_{\max} \leqslant \frac{1}{a_1(1-\alpha_1)} + \frac{1}{a_2(\alpha_2-1)}$, which is irrelevant to the initial state $x(t_0)$.*

Lemma 2 (Garg, Baranwal, Gupta, Vasudevan, & Panagou, 2019). *For any $c \in (0, 1)$, we have $\left(\frac{1-c}{1+c}\right)^{1-a} > c$, $a \in (1 - \mu(c), 1) \cup (1, +\infty)$ with $\mu(c) = \frac{\log(c)}{\log\left(\frac{1-c}{1+c}\right)}$.*

Definition 1 (RIP) (Candès, 2008). *The matrix satisfies the order-s-RIP condition if for any s-sparse vector $x \in R^n$ and $\eta_s \in (0, 1)$, one has*

$$(1 - \eta_s)\|x\|_2^2 \leqslant \|Ax\|_2^2 \leqslant (1 + \eta_s)\|x\|_2^2.$$

Downloaded from http://direct.mit.edu/neco/article-pdf/34/8/1727/2034959/neco_a_01508.pdf by HONG KONG POLYTECHNIC UNIVERSITY user on 13 August 2024

Lemma 3. *Let $g(x)$ be $\frac{1}{2}\|Ax-b\|_2^2$. With the help of 2s-RIP condition ($\eta_{2s} > 0$), $\nabla g(x) = A^T(Ax-b)$ satisfies the following Lipschitz continuity and strong-monotonicity:*

1. *The gradient ∇g has Lipschitz continuous of s-sparse vectors, given by*

$$\|\nabla g(x_1) - \nabla g(x_2)\|_2 \leqslant (1+\eta_{2s})\|x_1 - x_2\|_2. \tag{2.2}$$

2. *The ∇g satisfies the strong-monotonicity, that is, it follows that*

$$(x_1-x_2)^T(\nabla g(x_1) - \nabla g(x_2)) \geqslant (1-\eta_{2s})\|x_1-x_2\|_2^2, \tag{2.3}$$

where x_1 and $x_2 \in R^n$.

3 Neurodynamic Flows

We propose an FTSNF based on the proximal operator of model $L_{1-\beta 2}$, $\beta \in [0,1]$ to solve problem 2 to recover a sparse signal. Before giving the FTSNF, the necessary proximal operator of model $L_{1-\beta 2}$ needs to be given as follows:

Lemma 4. *The closed-form solution of the proximal operator to model $L_{1-\beta 2}$ with $\tau > 0, \lambda > 0, \beta \in [0,1]$ is*

$$\begin{aligned} &Prox_{\tau\lambda(\|\cdot\|_1-\beta\|\cdot\|_2)}(y) = \arg\min_{x\in R^n} \tau\lambda(\|x\|_1 - \beta\|x\|_2) + \frac{1}{2}\|x-y\|_2^2, \\ &= \begin{cases} sign(y) * max\{|y| - \tau\lambda, 0\}, & if\ \beta = 0, \\ sign(y) * max\{|y| - \tau\lambda, 0\} + \frac{\tau\lambda\beta sign(y) * max\{|y|-\tau\lambda,0\}}{\|sign(y) * max\{|y|-\tau\lambda,0\}\|_2}, & if\ \beta \in (0,1], \end{cases} \end{aligned} \tag{3.1}$$

where $*$ indicates the componentwise multiplication and $sign(y_i) = 1$, if $y_i > 0$; $sign(y_i) = -1$, if $y_i < 0$; $sign(y_i) = 0$, if $y_i = 0$, $i = 1, \ldots, n$.

Proof. The proof approach is inspired by the work in Qin and Lou (2019). Based on the KKT conditions, the optimal conditions of optimization problem $\min_x \tau\lambda(\|x\|_1 - \beta\|x\|_2) + \frac{1}{2}\|x-y\|_2^2$ with $x \neq \mathbf{0}$ satisfy

$$\operatorname{sign}(x_i)\left(\tau\lambda - \tau\lambda\beta\frac{|x_i|}{\|x\|_2}\right) + x_i = y_i, i = 1, \ldots, n, \tag{3.2}$$

with $\operatorname{sign}(x_i) = 1$, if $x_i > 0$; $\operatorname{sign}(x_i) = -1$, if $x_i < 0$; and $\operatorname{sign}(x_i) = \frac{y_i}{\lambda\tau} \in [-1,1]$, if $x_i = 0$.

We will prove that equation 3.1 holds in the following two cases:

Case 1: $\beta = 0$. Since $x_i = \operatorname{sign}(x_i)|x_i|$, the optimal conditions, equation 3.2, become

$$\operatorname{sign}(x_i)(\tau\lambda + |x_i|) - y_i = 0, i = 1, \ldots, n.$$

Downloaded from http://direct.mit.edu/neco/article-pdf/34/8/1727/2034959/neco_a_01508.pdf by HONG KONG POLYTECHNIC UNIVERSITY user on 13 August 2024

I: $|x_i| > 0$ and $\tau, \lambda > 0$ imply $\text{sign}(x_i) = \text{sign}(y_i)$ and $\tau\lambda + |x_i| = |y_i|$.
  1: $|y_i| > \tau\lambda$, one has $|x_i| = |y_i| - \tau\lambda$ which means $x_i = \text{sign}(x_i)(|y_i| - \tau\lambda) = \text{sign}(y_i)(|y_i| - \tau\lambda)$.
  2: $|y_i| \leqslant \tau\lambda$ does not exist.

II: $|x_i| = 0$, the optimal conditions, equation 3.2, reduce to $\text{sign}(0)\,\tau\lambda = y_i$, that is, $\text{sign}(0) = \frac{y_i}{\tau\lambda}$. Since $|y_i| = \text{sign}(y_i)\, y_i$, one has $|y_i| = \tau\lambda\,\text{sign}(0) * \text{sign}\big(\tau\lambda\,\text{sign}(0)\big)$.
  1: Since $\tau, \lambda > 0$, then $\text{sign}(0)$ and $\text{sign}\big(\text{sign}(0)\,\tau\lambda\big)$ have the same positive and negative signs. Note that $-1 \leqslant \text{sign}(0) \leqslant 1$, $-1 \leqslant \text{sign}\big(\text{sign}(0)\,\tau\lambda\big) \leqslant 1$, and we further obtain $|y_i| \leqslant \tau\lambda$.
  2: $|y_i| > \tau\lambda$ does not exist.

To sum up and provide a unified form, we have

$$\begin{aligned} x_i &= \begin{cases} \text{sign}(y_i)(|y_i| - \tau\lambda), & \text{if } |y_i| - \tau\lambda > 0 \\ 0, & \text{if } |y_i| - \tau\lambda \leqslant 0 \end{cases} \\ &= \text{sign}(y_i)\max\big\{|y_i| - \tau\lambda, 0\big\}, i = 1, \ldots, n. \\ \Rightarrow\ x &= \text{sign}(y) * \max\big\{|y| - \tau\lambda, 0\big\}. \end{aligned} \tag{3.3}$$

Thus, the classical soft-thresholding operator of the L_1-norm can be achieved in equation 3.3 as $\tau = 1$.

Next, we construct the closed-form solution of the proximal operator for model $L_{1-\beta 2}$ with $\tau > 0, \lambda > 0, \beta \in (0, 1]$ based on the proximal operator of the L_1-norm.

Case 2: $\beta \in (0, 1]$. Equation 3.3 with $x_i = \text{sign}(x_i)\,|x_i|, i = 1, \ldots, n$ and $x \neq \mathbf{0}$ reduces to

$$\text{sign}(x_i)\left(\tau\lambda - \tau\lambda\beta\frac{|x_i|}{\|x\|_2} + |x_i|\right) = y_i, i = 1, \ldots, n. \tag{3.4}$$

I: Let $|x_i| > 0$. Combining this with $\beta \in (0, 1]$, we have $\tau\lambda - \tau\lambda\beta\frac{|x_i|}{\|x\|_2} + |x_i| \geqslant 0$ and $\text{sign}(x_i) = \text{sign}(y_i)$ from equation 3.4. Furthermore, we have $\tau\lambda - \tau\lambda\beta\frac{|x_i|}{\|x\|_2} + |x_i| = |y_i|$. According to section I in case 1, if we choose a function $x_i = \Psi(z_i)$ that can transform $\tau\lambda - \tau\lambda\beta\frac{|x_i|}{\|x\|_2} + |x_i| = |y_i|$ into

$$\tau\lambda + |z_i| = |y_i| \tag{3.5}$$

(i.e., letting $z_i = \text{sign}(y_i)\max\big\{|y_i| - \tau\lambda, 0\big\}, i = 1, \ldots, n$), then we establish the relationship between the proximal operator of the $L_{1-\beta 2}$ hybrid norm with $\tau > 0, \lambda > 0, \beta \in (0, 1]$ and the proximal operator of the L_1-norm.

Downloaded from http://direct.mit.edu/neco/article-pdf/34/8/1727/2034959/neco_a_01508.pdf by HONG KONG POLYTECHNIC UNIVERSITY user on 13 August 2024

Note that $\tau\lambda - \tau\lambda\beta\frac{|z_i|}{\|z\|_2} + |z_i|\left(1+\frac{\lambda\beta}{\|z\|_2}\right) = \tau\lambda + |z_i| = |y_i|$; then we can choose $x_i = \Psi(z_i)$ if it satisfies the following conditions:

$$(1):\ \mathrm{sign}(x_i) = \mathrm{sign}(z_i),\ (2):\ |z_i|\left(1+\frac{\lambda\beta}{\|z\|_2}\right) = |x_i|,\ (3):\ \frac{|z_i|}{\|z\|_2} = \frac{|x_i|}{\|x\|_2}.$$

Let $x_i = \Psi(z_i) = z_i + \frac{\tau\lambda\beta z_i}{\|z\|_2}$, $|z_i| > 0$, $i = 1, \ldots, n$. Obviously, $\mathrm{sign}(z_i) = \mathrm{sign}(x_i)$ and $|x_i| = |z_i| + \frac{\tau\lambda\beta|z_i|}{\|z\|_2}$, $i = 1, \ldots, n$, that is, conditions 1 and 2 hold.

Note that $\|x\|_2 = \left(1+\frac{\tau\lambda\beta}{\|z\|_2}\right)\sqrt{\sum_{i=1}^{n}|z_i|^2} = \|z\|_2 + \tau\lambda\beta$. Then, $|x_i|$ divided by $\|x\|_2$ yields

$$\frac{|x_i|}{\|x\|_2} = \frac{|z_i|\left(1+\frac{\tau\lambda\beta}{\|z\|_2}\right)}{\|z\|_2 + \tau\lambda\beta} = \frac{|z_i|}{\|z\|_2},\ i = 1, \ldots, n,$$

which implies that condition 3 hold.

Combining $\mathrm{sign}(z_i) = \mathrm{sign}(x_i) = \mathrm{sign}(y_i)$ with $\tau\lambda - \tau\lambda\beta\frac{|x_i|}{\|x\|_2} + |x_i| = \tau\lambda - \tau\lambda\beta\frac{|z_i|}{\|z\|_2} + |z_i|\left(1+\frac{\tau\lambda\beta}{\|z\|_2}\right) = \tau\lambda + |z_i| = |b_i|$, $i = 1, \ldots, n$, the optimal condition 3.4 can be obtained as follows:

$$\begin{aligned} &Prox_{\tau\lambda(\|\cdot\|_1 - \beta\|\cdot\|_2)}(y) = x = z + \frac{\tau\lambda\beta z}{\|z\|_2} \\ &= \mathrm{sign}(y) * \left(|y| - \tau\lambda\right) + \frac{\tau\lambda\beta\,\mathrm{sign}(y) * \left(|y| - \tau\lambda\right)}{\left\|\mathrm{sign}(y) * \left(|y| - \tau\lambda\right)\right\|_2},\ |y_i| > \tau\lambda,\ i = 1, \ldots, n. \end{aligned}$$

II: Let $|x_i| = 0$. The optimal condition 3.4 becomes $\tau\lambda\,\mathrm{sign}(0) = y_i$, $i = 1, \ldots, n$, which are similar to section II in case 1. It implies that $x_i = 0$ if $|y_i| \leqslant \tau\lambda$ with any $i = 1, \ldots, n$.

In conclusion, in a unified form, we deduce that

$$\begin{aligned} &Prox_{\tau\lambda(\|\cdot\|_1 - \beta\|\cdot\|_2)}(y) = x = z + \frac{\tau\lambda\beta z}{\|z\|_2} \\ &= \mathrm{sign}(y) * \max\{|y| - \tau\lambda, 0\} + \frac{\tau\lambda\beta\,\mathrm{sign}(y) * \max\{|y| - \tau\lambda, 0\}}{\|\mathrm{sign}(y) * \max\{|y| - \tau\lambda, 0\}\|_2}. \end{aligned} \tag{3.6}$$

Therefore, from cases 1 and 2, the proof is completed. □

Remark 1. Note that in the proof process, if $z_i = 0, y_i \neq 0, \lambda\tau\,\mathrm{sign}(z_i) = y_i$ implies that $\lambda\tau\,\mathrm{sign}(0) = \frac{y_i}{\lambda\tau} \neq 0 \in [-1, 1]$ if $y_i \neq 0$. However, in the practical calculation process, the ingenious unified form $\mathrm{sign}(y_i)\max\{|y_i|$

Downloaded from http://direct.mit.edu/neco/article-pdf/34/8/1727/2034959/neco_a_01508.pdf by HONG KONG POLYTECHNIC UNIVERSITY user on 13 August 2024

$-\tau\lambda, 0\}, i = 1, \ldots, n$ makes sign $(0) = 0$ since it occurs only in the following cases: $\max\left\{|y_i| - \tau\lambda, 0\right\} = 0$ if $|y_i| - \tau\lambda \leqslant 0$:

1. $0 < y_i < \tau\lambda, z_i = \max\left\{|y_i| - \tau\lambda, 0\right\} = 0.$
2. $-\tau\lambda < y_i < 0, z_i = -\max\left\{|y_i| - \tau\lambda, 0\right\} = 0.$
3. $y_i = 0, z_i = \text{sign}(0)\max\left\{|y_i| - \tau\lambda, 0\right\} = 0.$

Note that sign $(0) = \frac{y_i}{\lambda\tau} = 0$ since $y_i = 0$ in case 3. This explains why in the practical calculation process, we can choose the signum function as sign $(y_i) = 1$, if $y_i > 0$; sign $(y_i) = -1$, if $y_i < 0$; sign $(y_i) = 0$, if $y_i = 0$.

Thus, in lemma 4, the signum function is defined as sign $(v_i) = 1$ if $v_i > 0$; sign $(v_i) = -1$, if $v_i < 0$; and sign $(v_i) = \frac{y_i}{\lambda\tau}$, if $v_i = 0$ where the v_i can take x_i, z_i, and y_i.

The sign $(y_i) = 1$ if $y_i > 0$; sign $(y_i) = -1$ if $y_i < 0$; and sign $(y_i) = 0$, if $y_i = 0$ are special cases only when $v_i = y_i$. Since the proximal operator used in designing the neurodynamic flows or algorithms contains only sign (y_i), it can be defined as sign $(0) = 0$.

The proposed fixed-time stable neurodynamic flow (FTSNF) is

$$\begin{cases} \dot{x} = -\alpha\frac{x-h(x)}{\|x-h(x)\|_2^{1-a}} - \gamma\frac{x-h(x)}{\|x-h(x)\|_2^{1-b}}, & \text{if } x \in R^n \setminus FP(\bar{x}), \\ x = \bar{x}, & \text{otherwise,} \end{cases} \tag{3.7}$$

where $h(x) = Prox_{\tau\lambda(\|\cdot\|_1 - \beta\|\cdot\|_2)}\left(x - \tau A^T(Ax - b)\right)$, $FP(\bar{x}) = \left\{\bar{x} \in R^n | \bar{x} = h(\bar{x})\right\}$, $\tau, \lambda > 0, \alpha, \gamma > 0, a \in (0, 1), b > 1, \lambda > 0$ and $\beta \in [0, 1]$.

Note that the optimal condition of equation 1.2 becomes

$$\begin{aligned} &\mathbf{0} \in \partial\tau\lambda\|x^*\|_1 - \lambda\tau\beta\frac{x^*}{\|x^*\|_2} + \tau A^T(Ax^* - b) \\ &= A^T(Ax^* - b) - x^* + \text{diag}\left\{\text{sign}(x_1^*), \ldots, \text{sign}(x_n^*)\right\} \\ &\quad \times \left(\lambda\tau\mathbf{1} - \text{diag}\left\{\frac{\lambda\tau\beta x_1^*}{\|x^*\|_2} + |x_1^*|, \ldots, \frac{\lambda\tau\beta x_n^*}{\|x^*\|_2} + |x_n^*|\right\}\right) \\ &\Rightarrow x^* - \tau A^T(Ax^* - b) \in \text{diag}\left\{\text{sign}(x_1^*), \ldots, \text{sign}(x_n^*)\right\} \\ &\quad \times \left(\lambda\tau\mathbf{1} - \text{diag}\left\{\frac{\lambda\tau\beta x_1^*}{\|x^*\|_2} + |x_1^*|, \ldots, \frac{\lambda\tau\beta x_n^*}{\|x^*\|_2} + |x_n^*|\right\}\right). \end{aligned}$$

Note that $Prox_{\tau\lambda(\|\cdot\|_1 - \beta\|\cdot\|_2)} = (I + \partial\tau\lambda(\|\cdot\|_1 - \beta\|\cdot\|_2))^{-1}$ in equation 3.1. Thus, we obtain $x^* = Prox_{\tau\lambda(\|\cdot\|_1 - \beta\|\cdot\|_2)}\left(x^* - \tau A^T(Ax^* - b)\right)$, that is, the KKT point of problem 2 is the same as the fixed point of $h(x)$ (i.e., $h(x) = x$) and an equilibrium point of FTSNF, equation 3.7.

Downloaded from http://direct.mit.edu/neco/article-pdf/34/8/1727/2034959/neco_a_01508.pdf by HONG KONG POLYTECHNIC UNIVERSITY user on 13 August 2024

Theorem 1. *Under the assumptions that* $\lambda \in \left(0, \frac{1-\eta_{2s}}{\beta \mathfrak{l}_{\|\cdot\|_2}}\right)$ *and* $\tau \in \left(0, \frac{2\left(1-\eta_{2s}-\lambda\beta \mathfrak{l}_{\|\cdot\|_2}\right)}{\left(1+\eta_{2s}\right)^2}\right)$, *$x^*$ is an equilibrium point (i.e., it satisfies the above KKT condition) of problem 2. Then we obtain*

$$\|h(x) - x^*\|_2 \leqslant \mathfrak{c}\|x - x^*\|_2, \tag{3.8}$$

with $\mathfrak{c} \in (0, 1)$.

Proof. Let $g(x) = \frac{1}{2}\|Ax - b\|_2^2$, $f(x) = \lambda(\|x\|_1 - \beta\|x\|_2)$, $h(x) = prox_{\tau f}(x - \tau\nabla g(x))$, and let $y \in R^n$. Suppose that $p_\theta = \theta y + (1-\theta)h(x)$, and set $\theta \in (0, 1)$; then one has

$$\begin{aligned}
&\tau f(h(x)) \\
\leqslant\ & \tau f(p_\theta) + \frac{1}{2}\|x - \tau\nabla g(x) - p_\theta\|_2^2 - \frac{1}{2}\|x - \tau\nabla g(x) - h(x)\|_2^2 \\
=\ & \tau\lambda\left(\left\|\theta y + (1-\theta)h(x)\right\|_1 - \beta\left\|\theta y + (1-\theta)h(x)\right\|_2\right) \\
& + \frac{1}{2}\left\|x - \tau\nabla g(x) - h(x) + \theta h(x) - \theta y\right\|_2^2 - \frac{1}{2}\left\|x - \tau\nabla g(x) - h(x)\right\|_2^2 \\
\leqslant\ & \theta\lambda\tau\|y\|_1 + (1-\theta)\lambda\tau\|h(x)\|_1 + \frac{\theta^2}{2}\|y - h(x)\|_2^2 \\
& - \theta(y - h(x))^T(x - \tau\nabla g(x) - h(x)) - \lambda\beta\theta\tau\|y\|_2 \\
& - \lambda\beta(1-\theta)\tau\|h(x)\|_2 + \frac{\tau\lambda\theta\beta(1-\theta)\mathfrak{l}_{\|\cdot\|_2}}{2}\|h(x) - y\|_2^2 \\
=\ & \tau\theta f(y) + \tau(1-\theta)f(h(x)) - \theta(y - h(x))^T(x - \tau\nabla g(x) - h(x)) \\
& + \frac{\tau\lambda\theta\beta(1-\theta)\mathfrak{l}_{\|\cdot\|_2}}{2}\|h(x) - y\|^2 + \frac{\theta^2}{2}\|y - h(x)\|_2^2 \\
\Rightarrow\ & \tau f(h(x)) \leqslant \tau f(y) - (y - h(x))^T(x - \tau\nabla g(x) - h(x)) \\
& + \frac{\lambda\tau\beta\mathfrak{l}_{\|\cdot\|_2}(1-\theta) + \theta}{2}\|h(x) - y\|_2^2,
\end{aligned} \tag{3.9}$$

where the first inequality holds from the property of the proximal operator to model $L_{1-\beta 2}$, $\beta \in [0, 1]$ and the second inequality holds from the convexity inequality of function $\|\cdot\|_1$:

$$\tau\lambda\theta\left\|\theta y + (1-\theta)h(x)\right\|_1 \leqslant \theta\lambda\tau\left\|y\right\|_1 + (1-\theta)\lambda\tau\left\|h(x)\right\|_1,$$

and the Lipschitz property of $\frac{1}{2}\|\cdot\|_2^2$:

$$\frac{1}{2}\left\|x - \tau\nabla g(x) - h(x) + \theta h(x) - \theta y\right\|_2^2 - \frac{1}{2}\left\|x - \tau\nabla g(x) - h(x)\right\|_2^2$$

Downloaded from http://direct.mit.edu/neco/article-pdf/34/8/1727/2034959/neco_a_01508.pdf by HONG KONG POLYTECHNIC UNIVERSITY user on 13 August 2024

$$\leqslant \theta\left(x-\tau\nabla g(x)-h(x)\right)^T\left(h(x)-y\right)+\frac{1}{2}\left\|\theta h(x)-\theta y\right\|_2^2$$
$$=-\theta\left(x-\tau\nabla g(x)-h(x)\right)^T\left(y-h(x)\right)+\frac{\theta^2}{2}\left\|h(x)-y\right\|_2^2,$$

and the concavity of $-\|\cdot\|_2$ with a Lipschitz constant $\mathfrak{l}_{\|\cdot\|_2}$ of its gradient:

$$-\lambda\tau\beta\left\|\theta y+(1-\theta)h(x)\right\|_2$$
$$\leqslant -\lambda\tau\beta\left\|y\right\|_2-\lambda\tau\beta(1-\theta)\left\|h(x)\right\|_2+\frac{\tau\lambda\theta\beta(1-\theta)L_{\|\cdot\|_2}}{2}\left\|h(x)-y\right\|^2.$$

Letting $\theta\to 0$, equation 3.9 becomes

$$\left(y-h(x)\right)^T\left(h(x)-(x-\tau\nabla g(x))\right)$$
$$+\frac{\tau\lambda\beta\mathfrak{l}_{\|\cdot\|_2}}{2}\|h(x)-y\|_2^2\geqslant\tau\left(f(h(x))-f(y)\right).\tag{3.10}$$

In particular, let $y=x^*$; then equation 3.10 becomes

$$\left(x^*-h(x)\right)^T\left(h(x)-x\right)+\frac{\tau\lambda\beta\mathfrak{l}_{\|\cdot\|_2}}{2}\|h(x)-x^*\|_2^2$$
$$\geqslant\tau\left(f(h(x))-f(x^*)\right)-\tau\nabla g(x)^T\left(x^*-h(x)\right).\tag{3.11}$$

Furthermore, using the Lipschitz property of $-\frac{\cdot}{\|\cdot\|_2}$ and convexity of $\|\cdot\|_1$, we have

$$\tau\left(f(h(x))-f(x^*)\right)\geqslant\tau\partial f(x^*)^T\left(h(x)-x^*\right)-\frac{\tau\lambda\beta\mathfrak{l}_{\|\cdot\|_2}}{2}\|x^*-h(x)\|_2^2.\tag{3.12}$$

In addition, the optimal point x^* satisfies the following variational inequality:

$$\lambda\left(h(x)-x^*\right)^T\left(\partial f(x^*)+\nabla g(x^*)\right)\geqslant 0,\forall h(x)\in R^n.\tag{3.13}$$

Combining equations 3.12 and 3.13, equation 3.11 becomes

$$\left(h(x)-x\right)^T\left(x^*-h(x)\right)\geqslant\tau\left(\nabla g(x)-\nabla g(x^*)\right)^T\left(h(x)-x^*\right)$$
$$-\tau\lambda\beta\mathfrak{l}_{\|\cdot\|_2}\|x^*-h(x)\|_2^2.\tag{3.14}$$

Rearrange equation 3.14 as follows:

$$\left(x-h(x)\right)^T\left(x^*-h(x)\right)$$
$$\leqslant\lambda\tau\beta\mathfrak{l}L_{\|\cdot\|_2}\|x^*-h(x)\|_2^2+\tau\left(\nabla g(x^*)-\nabla g(x)\right)^T\left(h(x)-x^*\right)$$

Downloaded from http://direct.mit.edu/neco/article-pdf/34/8/1727/2034959/neco_a_01508.pdf by HONG KONG POLYTECHNIC UNIVERSITY user on 13 August 2024

$$
\begin{aligned}
&= \lambda\tau\beta\mathfrak{l}_{\|\cdot\|_2}\|x^* - h(x)\|_2^2 + \tau\left(\nabla g(x^*) - \nabla g(h(x))\right)^T\left(h(x) - x^*\right)\\
&\quad + \tau\left(\nabla g(h(x)) - \nabla g(x)\right)^T\left(h(x) - x^*\right)\\
&\leqslant -\tau\left(1 - \eta_{2s}\right)\|h(x) - x^*\|_2^2 + \frac{\tau^2\left(1+\eta_{2s}\right)^2}{2}\|h(x) - x^*\|_2^2\\
&\quad + \frac{1}{2}\|h(x) - x\|_2^2 + \lambda\tau\beta\mathfrak{l}_{\|\cdot\|_2}\|x^* - h(x)\|_2^2, \qquad (3.15)
\end{aligned}
$$

where the last inequality holds from the following conditions:

$$
\begin{aligned}
&\textbf{(i)} \quad \tau\left(\nabla g(x^*) - \nabla g(h(x))\right)^T\left(h(x) - x^*\right) \leqslant -\tau\left(1 - \eta_{2s}\right)\|h(x) - x^*\|_2^2,\\
&\textbf{(ii)} \quad \tau\left(\nabla g(h(x)) - \nabla g(x)\right)^T\left(h(x) - x^*\right) \leqslant \frac{\tau^2\left(1+\eta_{2s}\right)^2}{2}\|h(x) - x^*\|^2\\
&\qquad + \frac{1}{2}\|h(x) - x\|_2^2.
\end{aligned}
$$

Furthermore, note that

$$
\begin{aligned}
&\left(x - h(x)\right)^T\left(x^* - h(x)\right)\\
&= \frac{1}{2}\|x - h(x)\|_2^2 + \frac{1}{2}\|x^* - h(x)\|_2^2 - \frac{1}{2}\|x^* - x\|_2^2. \qquad (3.16)
\end{aligned}
$$

From both equations 3.15 and 3.16, it yields

$$
\begin{aligned}
&\|x - h(x)\|_2^2 + \|x^* - h(x)\|_2^2 - \|x^* - x\|_2^2\\
&\leqslant -2\tau\left(1 - \eta_{2s}\right)\|h(x) - x^*\|_2^2 + \tau^2\left(1+\eta_{2s}\right)^2\|h(x) - x^*\|_2^2\\
&\quad + \|h(x) - x\|_2^2 + 2\tau\lambda\beta\mathfrak{l}_{\|\cdot\|_2}\|x^* - h(x)\|_2^2\\
&\Rightarrow \left(1 + 2\tau\left(1 - \eta_{2s}\right) - \tau^2\left(1+\eta_{2s}\right)^2 - 2\tau\lambda\beta\mathfrak{l}_{\|\cdot\|_2}\right)\|x^* - h(x)\|_2^2 \leqslant \|x^* - x\|_2^2, \qquad (3.17)
\end{aligned}
$$

which implies that

$$
\|x^* - h(x)\|_2^2 \leqslant C\|x^* - x\|_2^2, \qquad (3.18)
$$

with $C = \frac{1}{1+2\tau(1-\eta_{2s})-\tau^2(1+\eta_{2s})^2-2\tau\lambda\beta\mathfrak{l}_{\|\cdot\|_2}}$. Note that $C \in (0,1)$ if $\tau \in \left(0, \frac{2\left(1-\eta_{2s}-\lambda\beta\mathfrak{l}_{\|\cdot\|_2}\right)}{\left(1+\eta_{2s}\right)^2}\right)$, $\lambda \in \left(0, \frac{1-\eta_{2s}}{\beta\mathfrak{l}_{\|\cdot\|_2}}\right)$. Thus, inequality 3.18 further implies that

$$
\|x^* - h(x)\|_2 \leqslant \mathfrak{c}\|x^* - x\|_2, \qquad (3.19)
$$

with $\mathfrak{c} = \sqrt{C} \in (0,1)$. □

Downloaded from http://direct.mit.edu/neco/article-pdf/34/8/1727/2034959/neco_a_01508.pdf by HONG KONG POLYTECHNIC UNIVERSITY user on 13 August 2024

The following theorem illustrates that the proposed FTSNF, equation 3.7, has a fixed-time convergence rate:

Theorem 2. *If* $\tau \in \left(0, \frac{2\left(1-\eta_{2s}-\lambda\beta\mathfrak{l}_{\|\cdot\|_2}\right)}{\left(1+\eta_{2s}\right)^2}\right)$, $\lambda \in \left(0, \frac{1-\eta_{2s}}{\beta\mathfrak{l}_{\|\cdot\|_2}}\right)$ *and* x^* *is a KKT point of problem 2, then there exists a constant* $\mu > 0$ *and* $a \in (1-\mu, 1) \cup (1, +\infty)$ *and* $b > 1$, *such that the proposed FTSNF, equation 3.7, is globally convergent in fixed time, that is, for any initial values, there exists a time budget*

$$T_{\max} = \frac{1}{2^{\frac{1+a}{2}} \frac{\alpha}{(1-\mathfrak{c})^{1-a}} \left(\left(\frac{1-\mathfrak{c}}{1+\mathfrak{c}}\right)^{1-a} - \mathfrak{c}\right)\left(\frac{1-a}{2}\right)} + \frac{1}{2^{\frac{1+b}{2}} \left(\frac{\gamma}{(1-\mathfrak{c})^{1-b}} \left(\left(\frac{1-\mathfrak{c}}{1+\mathfrak{c}}\right)^{1-b} - \mathfrak{c}\right)\right)\left(\frac{b-1}{2}\right)},$$

such that

$$\begin{cases} \frac{1}{2}\|x(t) - x^*\|_2^2 \geqslant 0, & t \leqslant T_{\max}, \\ \frac{1}{2}\|x(t) - x^*\|_2^2 = 0, & t > T_{\max}. \end{cases} \tag{3.20}$$

Proof. Consider a candidate Lyapunov function as follows:

$$V(x) = \frac{1}{2}\|x - x^*\|_2^2. \tag{3.21}$$

x^* is an optimal point that satisfies the KKT condition of problem 2. $V(x)$ is positive definite and radially unbounded. Then the derivative of $V(x)$ along with the trajectory of equation 3.7 from initial point $x(t_0) \setminus \{x^*\}$ is computed as

$$\begin{aligned} &\dot{V}(x) = (x - x^*)^T \dot{x} \\ &= (x - x^*)^T \left(-\alpha \frac{x - h(x)}{\|x - h(x)\|_2^{1-a}} - \gamma \frac{x - h(x)}{\|x - h(x)\|_2^{1-b}}\right) \\ &\leqslant -\alpha \frac{\|x - x^*\|_2^2}{\|x - h(x)\|_2^{1-a}} - \gamma \frac{\|x - x^*\|_2^2}{\|x - h(x)\|_2^{1-b}} \\ &\quad + \alpha \frac{\|x^* - h(x)\|_2 \|x - x^*\|_2}{\|x - h(x)\|_2^{1-a}} - \gamma \frac{\|x^* - h(x)\|_2 \|x - x^*\|_2}{\|x - h(x)\|_2^{1-b}}, \end{aligned} \tag{3.22}$$

where the inequality is established by the Cauchy-Schwarz inequality. From theorem 1 and $\tau \in \left(0, \frac{2\left(1-\eta_{2s}-\lambda\beta\mathfrak{l}_{\|\cdot\|_2}\right)}{\left(1+\eta_{2s}\right)^2}\right)$, $\lambda \in \left(0, \frac{1-\eta_{2s}}{\beta\mathfrak{l}_{\|\cdot\|_2}}\right)$, we have

$$\begin{aligned} &\|x - h(x)\|_2 \leqslant (1 + \mathfrak{c})\|x - x^*\|_2, \\ &\|x - h(x)\|_2 \geqslant (1 - \mathfrak{c})\|x - x^*\|_2. \end{aligned} \tag{3.23}$$

Downloaded from http://direct.mit.edu/neco/article-pdf/34/8/1727/2034959/neco_a_01508.pdf by HONG KONG POLYTECHNIC UNIVERSITY user on 13 August 2024

With the help of inequalities in equation 3.23, we deduce that

$$\begin{aligned}\dot{V}(x) &\leqslant -\alpha\frac{\|x-x^*\|_2^2}{(1+\mathfrak{c})^{1-a}\|x-x^*\|_2^{1-a}}-\gamma\frac{\|x-x^*\|_2^2}{(1+\mathfrak{c})^{1-a}\|x-x^*\|_2^{1-b}}\\&\quad+\alpha\frac{\mathfrak{c}\|x-x^*\|_2^2}{(1-\mathfrak{c})^{1-a}\|x-x^*\|_2^{1-a}}-\gamma\frac{\|x-x^*\|_2^2}{(1+\mathfrak{c})^{1-b}\|x-x^*\|_2^{1-b}}\\&=-u(a)\|x-x^*\|_2^{1+a}-\upsilon(b)\|x-x^*\|_2^{1+b},\end{aligned}\tag{3.24}$$

with $u(a)=\frac{\alpha}{(1-\mathfrak{c})^{1-a}}\left(\left(\frac{1-\mathfrak{c}}{1+\mathfrak{c}}\right)^{1-a}-\mathfrak{c}\right)$ and $\upsilon(b)=\frac{\gamma}{(1-\mathfrak{c})^{1-b}}\left(\left(\frac{1-\mathfrak{c}}{1+\mathfrak{c}}\right)^{1-b}-\mathfrak{c}\right)$. Therefore, equation 3.24 can be rewritten as

$$\dot{V}(x)\leqslant-\left(2^{\frac{1+a}{2}}u(a)V(x)^{\frac{1+a}{2}}+2^{\frac{1+b}{2}}\upsilon(b)V(x)^{\frac{1+b}{2}}\right).\tag{3.25}$$

From lemma 3 (i.e., $\exists\ \mu(\mathfrak{c})=\frac{\log(\mathfrak{c})}{\log\left(\frac{1-\mathfrak{c}}{1+\mathfrak{c}}\right)}>0$), $u(a)>0$ when $a\in(1-\mu,1)\cup(1,+\infty)$ and $\upsilon(b)>0$. In addition, we obtain $\frac{1+a}{2}\in(0.5,1)$ and $\frac{1+b}{2}>1$. According to the time budget of fixed-time convergence in number 2 in the list in lemma 1, the upper bound of the time budget $T_{\max}$ can be evaluated as

$$\begin{aligned}T_{\max}&=\frac{1}{2^{\frac{1+a}{2}}\frac{\alpha}{(1-\mathfrak{c})^{1-a}}\left(\left(\frac{1-\mathfrak{c}}{1+\mathfrak{c}}\right)^{1-a}-\mathfrak{c}\right)\left(\frac{1-a}{2}\right)}\\&\quad+\frac{1}{2^{\frac{1+b}{2}}\left(\frac{\gamma}{(1-\mathfrak{c})^{1-b}}\left(\left(\frac{1-\mathfrak{c}}{1+\mathfrak{c}}\right)^{1-b}-\mathfrak{c}\right)\right)\left(\frac{b-1}{2}\right)}.\end{aligned}\tag{3.26}$$

□

Remark 2. Compared with the L_1 model (i.e., $L_{1-\beta 2}$, $\beta=0$ in this letter), the $L_{1-\beta 2}$, $\beta\in(0,1]$ model has the following properties:

1. The model $L_{1-\beta 2}$, $\beta\in(0,1]$ is nonconvex, nonsmooth and Lipschitz.
2. The optimization problem for $L_{1-\beta 2}$, $\beta\in(0,1]$ is also called the difference-of-convex optimization problem.

Compared with the L_1 model ($L_{1-\beta 2}$, $\beta=0$) and for solving problem $L_{1-\beta 2}$, $\beta\in(0,1]$ there exist four difficulties:

1. The model $L_{1-\beta 2}$, $\beta\in(0,1]$ is nonconvex, and a novel method needs to be proposed for obtaining the closed-form solution of the proximal operator to the $L_{1-\beta 2}$, $\beta\in(0,1]$ hybrid norm, since the approach to derive the closed-form solution of the proximal operator of the convex function L_1 model is not applicable.
2. Designing neurodynamic flow with fixed-time convergence is more difficult. Note that theorem 1 is an essential result for deriving the fixed-time convergence of the FTSNF. This is totally different from

Downloaded from http://direct.mit.edu/neco/article-pdf/34/8/1727/2034959/neco_a_01508.pdf by HONG KONG POLYTECHNIC UNIVERSITY user on 13 August 2024

Garg and Baranwal (2020) and Garg et al. (2019). We obtain the time budget of fixed-time convergence 3.10 based on equation 3.9 only with Lipschitz and concave function properties of $-\|x\|_2$. This is useful in deriving the convergence property of the FTSNF for nonconvex $L_{1-\beta 2}$. However, it cannot be achieved from the research in Garg and Baranwal (2020) and Garg et al. (2019) because their results require that the function be convex.

3. Moreover, in Garg and Baranwal (2020) and Garg et al. (2019), the mixed variational inequalities (MVI) for convex functions are used. However, it is not suitable for our work, so we use the more generalized variational inequality, equation 3.13 to replace it;
4. When $\beta = 0$, the proposed FTSNF reduces to CAPPA in Garg and Baranwal (2020), that is, CAPPA is just one of the most particular (convex) cases of FTSNF.

4 Some Corollaries of FTSNF

Corollary 1. *Note that when $\beta = 0$, optimization problem 2 is transformed into the classical Lasso problem in Yu et al. (2017), Ren et al. (2019), Wen et al. (2020), and Garg and Baranwal (2020) (it is a convex optimization problem). Then the proposed FTSNF reduces to CAPPA (Garg & Baranwal, 2020) as follows:*

$$\begin{cases} \dot{x} = -\alpha \frac{x-h(x)}{\|x-h(x)\|_2^{1-a}} - \gamma \frac{x-h(x)}{\|x-h(x)\|_2^{1-b}}, & \text{if } x \in R^n \setminus FP(\bar{x}), \\ x = \bar{x}, & \text{otherwise}, \end{cases} \tag{4.1}$$

with $FP(\bar{x}) = \left\{\bar{x} \in R^n | \bar{x} = h(\bar{x})\right\}$, $h(x) = prox_{\tau\lambda(\|\cdot\|_1)}\left(x - \tau A^T (Ax - b)\right)$.

Corollary 2. *The proposed FTSNF, equation 3.7, has the following exponential convergence and finite time convergence rates when specific parameters are chosen as follows:*

1. ***Exponential convergence**: Let $a = 1, b = 1, \alpha, \gamma > 0$. FTSNF equation 3.7, reduces to*

$$\dot{x} = -(\alpha + \gamma)(x - h(x)), \tag{4.2}$$

with an exponential convergence rate (EPNF in this letter), that is, $\|x(t) - x^*\|_2^2 \leqslant \exp(-2(\gamma + \alpha)(1 - \mathfrak{c}))\|x(t_0) - x^*\|_2^2$.

2. ***Finite-time convergence**: Set $a \in (1 - \mu, 1) \cup (1, +\infty)$, $\alpha > 0$ and $\gamma = 0$. Then, FTSNF, equation 3.7, becomes*

$$\begin{cases} \dot{x} = -\alpha \frac{x-h(x)}{\|x-h(x)\|_2^{1-a}}, & \text{if } x \in R^n \setminus FP(\bar{x}), \\ x = \bar{x}, & \text{otherwise}. \end{cases} \tag{4.3}$$

Downloaded from http://direct.mit.edu/neco/article-pdf/34/8/1727/2034959/neco_a_01508.pdf by HONG KONG POLYTECHNIC UNIVERSITY user on 13 August 2024

The neurodynamic flow, equation 4.3, globally converges to a KKT point of problem 2 in finite time (we name it FPNF).

Proof. 1 According to equation 3.24, we have

$$\dot{V}(x) \leqslant -(\gamma+\alpha)(1-\mathfrak{c})\|x(t)-x^*\|_2^2 = -2(\gamma+\alpha)(1-\mathfrak{c})V(x),$$

which implies that $\|x(t)-x^*\|_2^2 \leqslant 2\exp(-2(\gamma+\alpha)(1-\mathfrak{c}))\|x(t_0)-x^*\|_2^2$.

2 Based on equations 3.24 and 3.25 and lemma 3, we obtain that

$$\dot{V}(x) \leqslant -(2)^{\frac{1+a}{2}} u(a) V^{\frac{1+a}{2}}(x), \tag{4.4}$$

with $u(a) = \frac{\alpha}{(1-\mathfrak{c})^{1-a}}\left(\left(\frac{1-\mathfrak{c}}{1+\mathfrak{c}}\right)^{1-a} - \mathfrak{c}\right)$.

From the Lipschitz continuity in point 1 in the numbered list in lemma 3, equation 4.4 achieves finite-time convergence with a time budget

$$T_{\max} = \|x(t_0)-x^*\|_2^{1-a} \frac{1}{(2)^{\frac{1+a}{2}} \frac{\alpha}{(1-\mathfrak{c})^{1-a}}\left(\left(\frac{1-\mathfrak{c}}{1+\mathfrak{c}}\right)^{1-a} - \mathfrak{c}\right)\left(\frac{1-a}{2}\right)}. \tag{4.5}$$

Note that the time budget in equation 4.5 of FPNF, equation 4.3, depends on the initial value $x(t_0)$, while the time budget in equation 3.26 of FTSNF equation 3.7 is independent of the initial value $x(t_0)$. □

5 Numerical Simulations

In this section, we present several experiments for recovering sparse signals to illustrate the effectiveness of the FTSNF, equation 3.7, and its variants (CAPPA, equation 4.1; EPNF, equation 4.2; and FPNF, equation 4.3). Their pseudocodes are given in algorithm 1.

5.1 Experiment 1. In this experiment, both orthonormal gaussian random matrix A and oversampled DCT matrix are used as the sensing matrix with $m = 40$, $n = 128$, where the oversampled DCT matrix is given by

$$A = [A_1, \ldots, A_n] \in R^{m\times n},$$

where $A_j = \frac{1}{\sqrt{n}}\cos\left(\frac{2\pi\omega j}{\Upsilon}\right)$, $j = 1, \ldots, n$, $\omega \in R^m$ is a random vector, and Υ the parameter is used to determine the matrix coherence. In addition, sparsity $s = 10$ is randomly determined, and the measurement $y \in R^m$ is collected by $\mathrm{b} = Ax + e$, where e is gaussian noise with standard derivation $\sigma = 0.01$. Moreover, the thresholds are $\lambda = \sigma\sqrt{2\log(n)}$, $\beta = 0.5$ and $\tau = 0.02$. We use ODE45 solver for simulation and generate necessary

Downloaded from http://direct.mit.edu/neco/article-pdf/34/8/1727/2034959/neco_a_01508.pdf by HONG KONG POLYTECHNIC UNIVERSITY user on 13 August 2024

Algorithm 1: Pseudocodes of FTSNF (equation 3.7), CAPPA (equation 4.1), EPNF (equation 4.2), and FPNF (equation 4.3).

Initialize Setting a, b, α, γ, x_0, e, σ, λ, β, τ, s and running time $[0, \mathcal{T}]$:
Getting orthonormal gaussian random matrix A

$$\begin{aligned} &\text{index} = \text{randperm}\,(n)\,, \text{index} = \text{index}\,(1:s)\,; \\ &B = \text{randn}\,(n,m)\,; A = \text{orth}\,(B)^{\mathrm{T}}\,; \\ &x_{\mathrm{s}} = \text{zero}\,(n,1)\,; x_{\mathrm{s}}\,(\text{index}) = \text{unifrnd}\,(-10,10,[s,1])\,; \\ &\varepsilon = \sigma \cdot \text{randn}\,(m,1)\,; \mathrm{b} = Ax + e. \end{aligned} \tag{5.1}$$

or getting oversampled DCT matrix A as follows:

$$\begin{aligned} &A = \text{zeros}\,(m,n)\,; \omega = \text{rand}\,(m,1)\,; \\ &\begin{cases} \text{for } j = 1:n; \\ A\,(:,j) = \frac{1.}{\text{sqrt}(n)} * \cos\,(2 * \pi * j * \omega./\Upsilon)\,; \\ \text{end.} \end{cases} \end{aligned} \tag{5.2}$$

Repeat $t \in [0, \mathcal{T}]$;
If $x_0 = h\,(x_0)$;
Return x_0.
Else: Running FTSNF (equation 3.7), CAPPA (equation 4.1), EPNF (equation 4.2), and FPNF (equation 4.3) according to the different relevant parameters by ODE45 in Matlab as follows:
1): when $\tau, \lambda > 0$, $\alpha, \gamma > 0$, $a \in (0,1)$, $b > 1$, $\lambda > 0$ and $\beta \in (0,1]$, running the FTSNF (12) with $h\,(x) = Prox_{\tau\lambda(\|\cdot\|_1 - \beta\|\cdot\|_2)}\left(x - \tau A^T\,(Ax - b)\right)$;
2): when $\tau, \lambda > 0$, $\alpha, \gamma > 0$, $a \in (0,1)$, $b > 1$, $\lambda > 0$ and $\beta = 0$, running CAPPA (4.1) with $h\,(x) = prox_{\tau\lambda(\|\cdot\|_1)}\left(x - \tau A^T\,(Ax - b)\right)$;
3): when $a = 1, b = 1, \alpha, \gamma > 0$, running the EPNF (equation 4.2);
4): when $a \in (1-\mu, 1) \cup (1, +\infty)$, $\alpha > 0$ and $\gamma = 0$, running the FPNF (equation 4.3);
Until $x\,(t) = h\,(x\,(t))$;
Return $x\,(t)$.

information through Matlab in the following way with orthonormal gaussian random matrix A.

First, the global stability performance of FTSNF, equation 3.7, for recovering a sparse signal is illustrated in Figure 1 (left) with various parameters of a, b under an orthonormal gaussian random matrix. Then we observe that FTSNF has a faster convergence rate when the parameters a and b are smaller (i.e., a lower fixed-time upper bound), which is displayed in Figure 1 (right). From Figure 2, we can see that the signals recovered by FTSNF (equation 3.7) with $a = 0.4$, $b = 1.4$; $a = 0.6$, $b = 1.6$, and $a = 0.8$, $b = 1.8$ are very close to the original sparse signal. Later, we compare the proposed FTSNF (equation 3.7) with fixed-time convergence, EPNF (equation 4.2) with exponential convergence and FPNF (equation 4.3) with finite-time convergence under oversampled DCT matrix A. From Figure 3 (left), we can see that FTSNF (equation 3.7) has a faster convergence rate than FPNF (equation 4.3) and EPNF (equation 4.2).

Downloaded from http://direct.mit.edu/neco/article-pdf/34/8/1727/2034959/neco_a_01508.pdf by HONG KONG POLYTECHNIC UNIVERSITY user on 13 August 2024

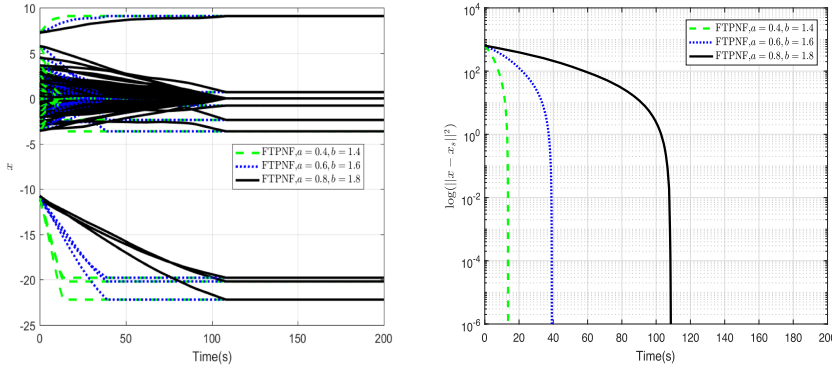

Figure 1: Gaussian random matrix: (Left) Transient behaviors of x by FTSNF 3.7. (Right) Log $\left(\|x - x_s\|_2^2\right)$.

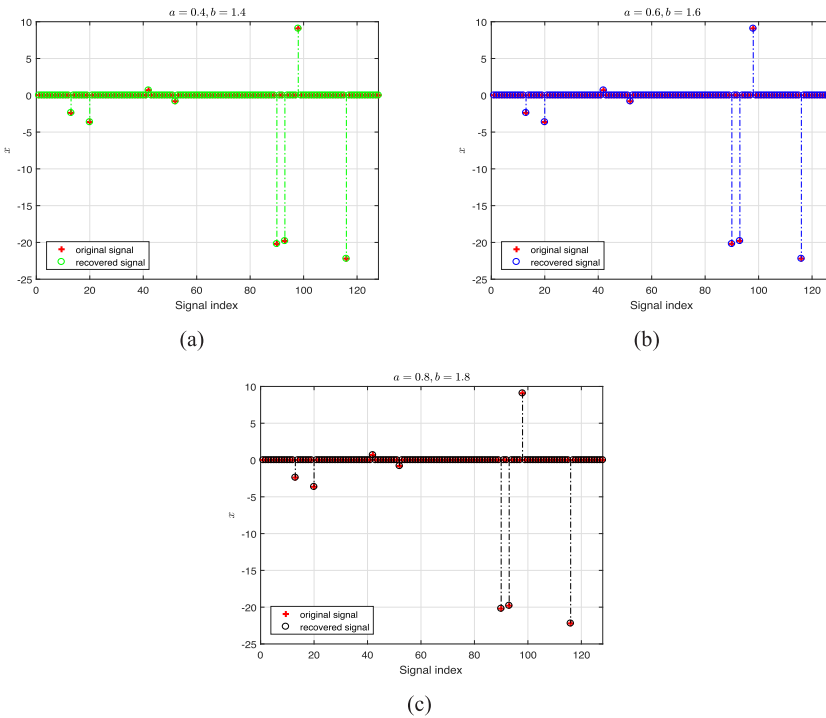

Figure 2: Gaussian random matrix: Recovered sparse signal by FTSNF (equation 3.7). (a) $a = 0.4$, $b = 1.4$. (b) $a = 0.6$, $b = 1.6$. (c) $a = 0.8$, $b = 1.8$.

Downloaded from http://direct.mit.edu/neco/article-pdf/34/8/1727/2034959/neco_a_01508.pdf by HONG KONG POLYTECHNIC UNIVERSITY user on 13 August 2024

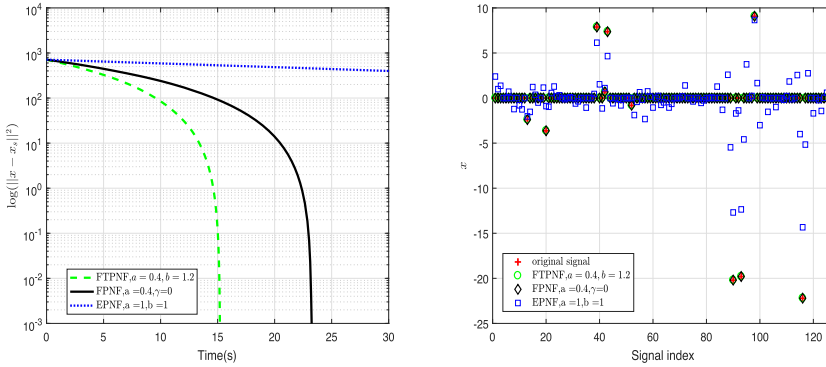

Figure 3: Oversampled DCT matrix, $\Upsilon = 3$. (Left) Log $\left(\|x - x_s\|_2^2\right)$. (Right) Recovered signals x of FTSNF (equation 3.7), EPNF (equation 4.2), and FPNF (equation 4.3) with the same parameters.

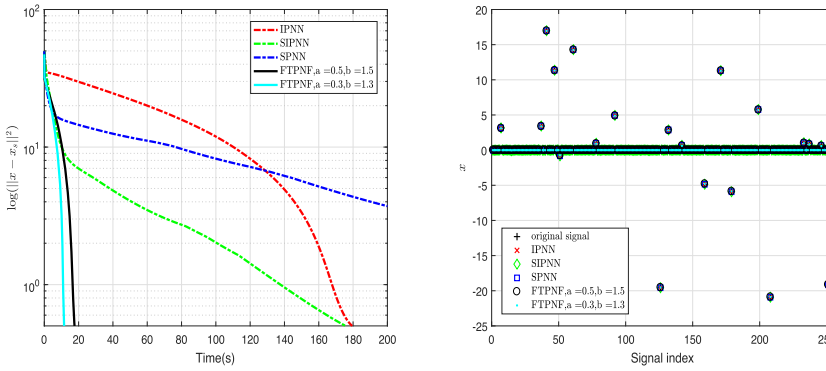

Figure 4: (Left) Log $\left(\|x - x_s\|_2^2\right)$. (Right) Recovered signals x.

Moreover, FPNF (equation 4.3) has a faster convergence rate than EPNF (equation 4.2). The recovered signals x by using FTSNF (equation 3.7), EPNF (equation 4.2), and FPNF (equation 4.3) with the same parameters are displayed in Figure 4 (right). Figure 4 (right) shows that recovered signals by using FTSNF (equation 3.7) and FPNF (equation 4.3) are very close to the original sparse signal. However, the recovered signal of EPNF (equation 4.2) has a large discrepancy with the original signal because of its relatively slow convergence rate, resulting in the desired results not being reached in the same amount of time.

5.2 Experiment 2. In this experiment, we compare the proposed FTSNF (equation 3.7) with IPNN (Zhu et al., 2018), SIPNN (Zhao et al., 2018) and

Downloaded from http://direct.mit.edu/neco/article-pdf/34/8/1727/2034959/neco_a_01508.pdf by HONG KONG POLYTECHNIC UNIVERSITY user on 13 August 2024

SPNN (Wang & Zhang, 2017) by solving the model with L_{1-2} and with noise measurement to recover the sparse signal with an orthonormal gaussian random matrix $A^{128\times256}$ and sparsity $s = 20$. Figure 4 shows the convergence rate and the recovered sparse signal. It can be seen from Figure 4 (left) that FTSNF (equation 3.7) has a faster convergence rate than the other approaches. In addition, SIPNN (Zhao et al., 2018) outperforms SPNN (Wang & Zhang, 2017) since an inertial term is added in SIPNN. Figure 4 (right) shows that FTSNF (equation 1.2), IPNN (Zhu et al., 2018), SIPNN (Zhao et al., 2018), and SPNN (Wang & Zhang, 2017) can effectively recover the sparse signal by solving the L_{1-2} hybrid norm minimization problem with noise measurement.

In addition, the proposed FTSNF (equation 3.7) with $a = 0.5, b = 1.5$, and $a = 0.3, b = 1.3$ in equation 4.3 are compared with PNNSR (Liu & Wang, 2016), PNNSR-finT (Wen et al., 2020), BP-LPNN (Feng et al., 2017), LCA (Balavoine et al., 2013), LCA-finT (Yu et al., 2017), LCA-fixT (Ren et al., 2019), and CAPPA (Garg & Baranwal, 2020) by solving the L_1-norm minimization problem (i.e., $L_{1-\beta 2}$, $\beta = 0$) with noise measurement (the standard derivation $\sigma = 0.02$), where $m = 128$, $n = 256$, and $s = 20$, to illustrate the effectiveness and superiority of FTSNF (equation 3.7). It can be seen from Figure 8 that the FTSNF (equation 3.7) with $a = 0.3, b = 1.3$ has the fastest convergence rate, and it also has the same convergence rate as CAPPA (Garg & Baranwal, 2020) when the same parameters $a = 0.5, b = 1.5$ are selected. This matches the conclusion of corollary 1. The PNNSR-finT (Wen et al., 2020), LCA-finT (Yu et al., 2017), and LCA-fixT (Ren et al., 2019) have faster convergence rates than their original neurodynamic flows PNNSR (Liu & Wang, 2016) and LCA (Balavoine et al., 2013) (neither of them introduces acceleration techniques). Figures 5 to 7 show the recovered sparse signal x by the neurodynamic flows already noted. Their recovered sparse signals are very close to the original sparse signal.

5.3 Experiment 3. Image reconstruction is widely used in engineering and scientific fields. In this example, we evaluate the proposed FTSNF (equation 3.7) by recovering a 256×256 "X-ray" image, as shown in Figure 9a. We use a discrete wavelet transform to obtain the sparse representation of the image and orthonormal gaussian random matrix in equation 5.1 as the sensing measurement A, and the measurement number $m = 150$ (i.e., $A \in R^{150\times256}$). Consider a gaussian white noise condition with noise level SNR = 10 dB (i.e., $\text{SNR} = 20\log_{10}\left(\frac{\|A\hat{x}-E\{A\hat{x}\}\|_2}{\|e\|_2}\right)$, where $\hat{x}$ denotes the original signal). The recovery performance is assessed by the peak signal-to-noise ratio (PSNR), which is $\text{PSNR} = 10\log_{10}\frac{255^2}{\text{MSE}}$ with $\text{MSE} = \frac{1}{n\times n}\sum_{i,j}(\hat{x}(i,j) - x(i,j))^2$, where $\hat{x}(i,j)$ and $x(i,j)$ are the pixels of the original image and the restored image, respectively. Figure 9 presents the recovery performance of the compared algorithms. It can be seen that FTSNF (equation 3.7) achieves the best performance. FTSNF (equation 3.7) and

Downloaded from http://direct.mit.edu/neco/article-pdf/34/8/1727/2034959/neco_a_01508.pdf by HONG KONG POLYTECHNIC UNIVERSITY user on 13 August 2024

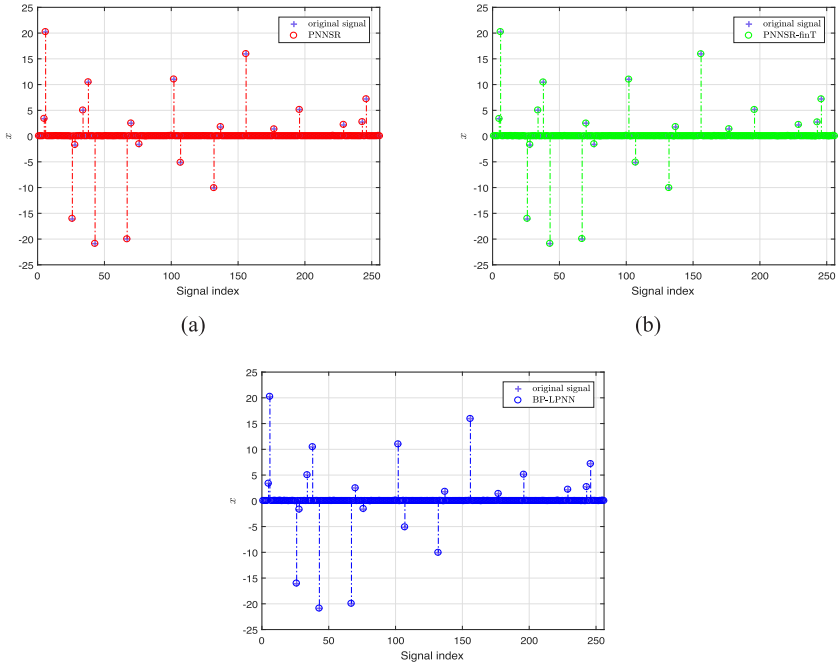

Figure 5: Recovered sparse signal. (a) PNNSR (Liu & Wang, 2016). (b) PNNSR-finT (Wen et al., 2020). (c) BP-LPNN (Feng et al., 2017).

L_{1-2}FBS (Lou & Yan, 2018) are better than OMP (Balavoine et al., 2013), Lasso–ADMM (Boyd, Parikh, Chu, Peleato, & Eckstein, 2011), and CAPPA (Garg & Baranwal, 2020). This is because the results of FTSNF (equation 3.7) and L_{1-2}FBS are obtained by solving the L_{1-2} hybrid norm, while the results of OMP, Lasso–ADMM and CAPPA are achieved by solving the L_1-norm model. In addition, it can be seen that CAPPA performs better than OMP and Lasso–ADMM. The experimental result in Figure 9 further demonstrates the effectiveness and superiority of the proposed FTSNF (equation 3.7).

6 Conclusion

This letter proposed a fixed-time stable neurodynamic flow (FTSNF) to deal with nonconvex $L_{1-\beta 2}, \beta \in (0, 1]$ hybrid norm and convex $L_{1-\beta 2}, \beta = 0$-norm minimization problems to capture sparse signals under RIP and noise measurement. First, a closed-form solution of the proximal operator to $L_{\tau\lambda(1-\beta 2)}, \tau, \lambda > 0, \beta \in [0, 1]$ was presented. Then we theoretically

Downloaded from http://direct.mit.edu/neco/article-pdf/34/8/1727/2034959/neco_a_01508.pdf by HONG KONG POLYTECHNIC UNIVERSITY user on 13 August 2024

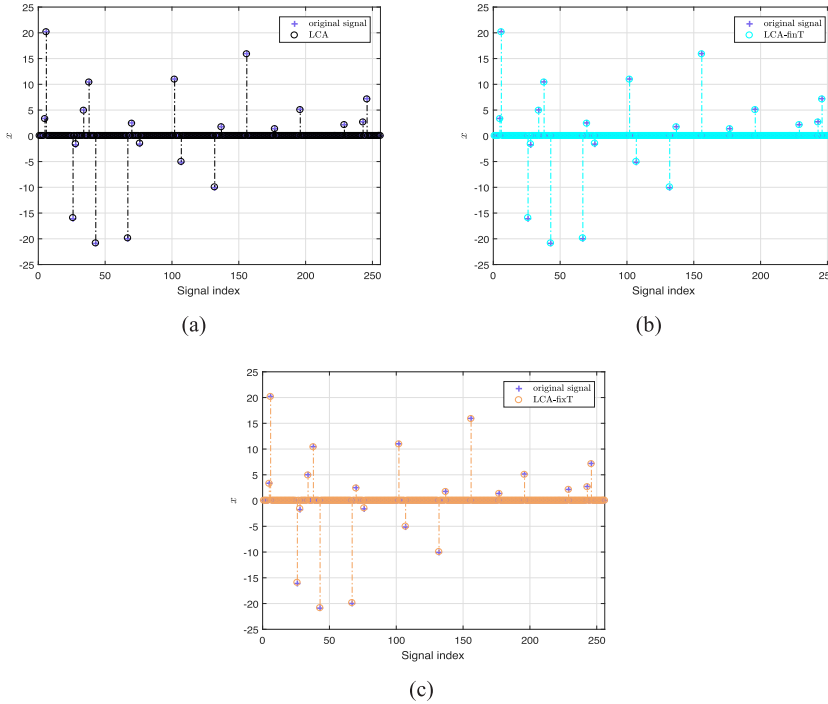

Figure 6: Recovered sparse signal. (a) LCA (Balavoine et al., 2013). (b) LCA-finT (Yu et al., 2017). (c) LCA-fixT (Ren et al., 2019).

proved that the fixed-time convergence property of the FTSNF converges to a KKT point of the nonconvex $L_{1-\beta 2}$ hybrid norm minimization problem (the uniquely optimal solution for the L_1-norm minimization problem is $\beta = 0$) without a convex hypothesis. We determined an upper bound of the time budget of the FTSNF. In addition, the FTSNF can be transformed into CAPPA when $\beta = 0$, EPNF with exponential convergence when $a = 1, b = 1, \alpha, \gamma > 0$, and FPNF with finite-time convergence when $a \in (1 - \mu, 1) \cup (1, +\infty), \alpha > 0$, and $\gamma = 0$. Finally, the feasibility and superiority of the proposed FTSNF were demonstrated by sparse signal recovery tests. It is well known that $L_{1-\beta 2}, \beta \in (0, 1]$ is nonconvex and nonsmooth but Lipschitz. However, many sparse signal recovery models are nonsmooth, nonconvex, and even non-Lipschitz in practice, such as the L_p-norm, L_{1-p} hybrid norm, and L_{p-q} hybrid norm. At present, the fast neurodynamic flows for solving these cases have not been extensively studied because they are more difficult due to their non-Lipschitz nature. Hence, designing neurodynamic flows with fixed-time convergence is the focus of our future research.

Downloaded from http://direct.mit.edu/neco/article-pdf/34/8/1727/2034959/neco_a_01508.pdf by HONG KONG POLYTECHNIC UNIVERSITY user on 13 August 2024

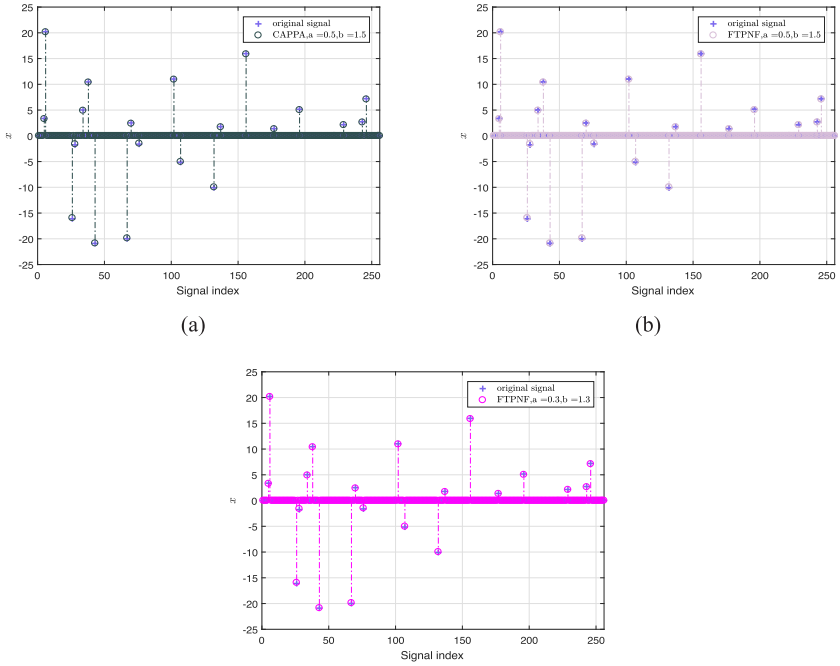

Figure 7: Recovered sparse signal. (a) CAPPA (Garg & Baranwal, 2020). (b) FTSNF (equation 3.7) $a = 0.5, b = 1.5$. (c) FTSNF (equation 3.7) $a = 0.3$, $b = 1.3$.

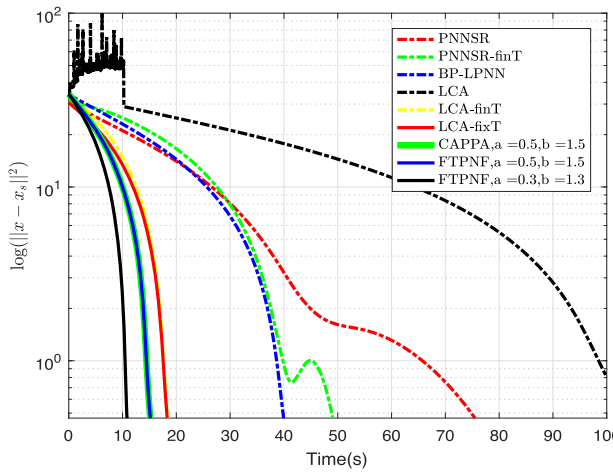

Figure 8: $\log\left(\|x - x_s\|_2^2\right)$.

Downloaded from http://direct.mit.edu/neco/article-pdf/34/8/1727/2034959/neco_a_01508.pdf by HONG KONG POLYTECHNIC UNIVERSITY user on 13 August 2024

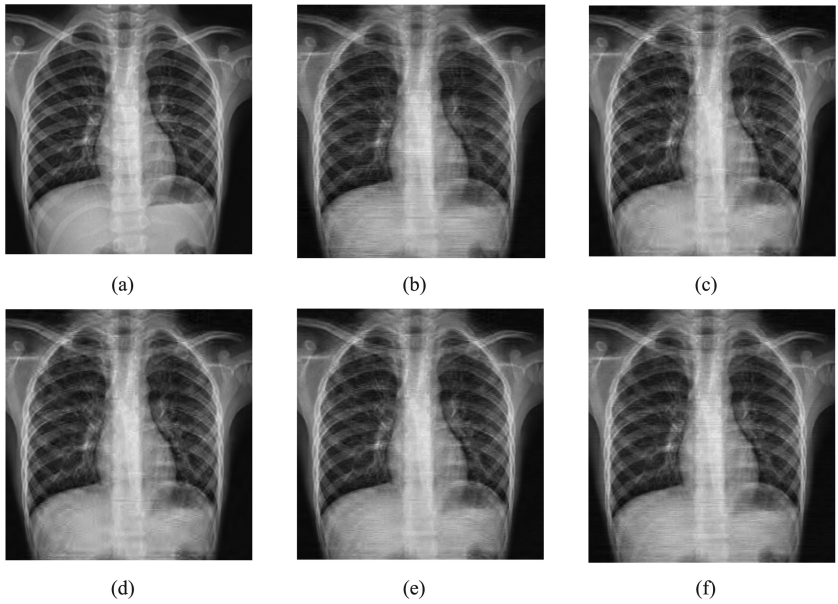

Figure 9: Image reconstruction. (a) Original image. (b) OPM (Balavoine et al., 2013), PSNR = 30.3304 dB. (c) Lasso–ADMM (Boyd, Parikh, Chu, Peleato, & Eckstein, 2011), PSNR = 30.5334 dB. (d) CAPPA (Garg & Baranwal, 2020) (i.e., FTSNF with $\beta = 0$), PSNR = 30.805 dB. (e) FTSNF(equation 3.7) PSNR = 32.3940 dB. (f) L_{1-2}FBS (Lou & Yan, 2018), PSNR = 31.888 dB.

Appendix

Definition 2. *System 3 has various stability concepts, as follows:*

- *(i)* ***Lyapunov stable around ϑ^*.*** *For any $\epsilon > 0$, there exists a $\rho(\epsilon) > 0$ such that $\|\vartheta(t) - \vartheta^*\|_2 < \epsilon$ when $\|\vartheta(t_0) - \vartheta^*\|_2 < \rho(\epsilon)$, for all $t > 0$. Then system is said to be Lyapunov stable around ϑ^*.*
- *(ii)* ***Globally asymptotically stable around ϑ^*.*** *If there exists $\rho(\epsilon) > 0$ and $\|\vartheta(t_0) - \vartheta^*\|_2 < \rho(\epsilon)$ exist such that $\lim_{t \to +\infty} \|\vartheta(t) - \vartheta^*\|_2 = 0$, then system 3 is called globally asymptotically stable around ϑ^*.*
- *(iii)* ***Globally exponentially stable around ϑ^*.*** *If system 3 is globally asymptotically stable and satisfies $\|\vartheta(t) - \vartheta^*\|_2 \leqslant \mathfrak{a} \exp(-\mathfrak{b}t) \|\vartheta(t_0) - \vartheta^*\|_2$ for all $t > 0$, where $\mathfrak{a}, \mathfrak{b} > 0$, then we call system 3 globally exponentially stable around ϑ^*.*
- *(iv)* ***Globally finite-time stable around ϑ^*.*** *If system 3 is globally stable, then there is a time budget $T_{\max}(x(t_0)) < +\infty$ of initial state x_0 such that $\|\vartheta(t) - \vartheta^*\|_2 = 0, t > T_{\max}(x(t_0))$. Then system 3 is known as globally finite-time stable around ϑ^*.*

Downloaded from http://direct.mit.edu/neco/article-pdf/34/8/1727/2034959/neco_a_01508.pdf by HONG KONG POLYTECHNIC UNIVERSITY user on 13 August 2024

(v) ***Globally fixed-time stable around ϑ^*.*** *If system 3 is globally stable, then there exists a time budget $T_{\max} < +\infty$ that is irrelevant to the initial state $x(t_0)$ such that $\|\vartheta(t) - \vartheta^*\|_2 = 0, t > T_{\max}$. Then system 3 is known as globally fixed-time stable around ϑ^*.*

Acknowledgments

This work was supported in part by the National Key R&D Program of China (grant 2018AAA0100101), in part by the National Natural Science Foundation of China (grants 61932006 and 62176027), in part by the Chongqing Technology Innovation and application development project, China (grant cstc2020jscx-msxmX0156), and in part by the Fundamental Research Funds for the Central Universities, China (project XDJK2020TY003).

References

Afonso, M. V., Bioucas-Dias, J. M., & Figueiredo, M. A. (2010). An augmented Lagrangian approach to the constrained optimization formulation of imaging inverse problems. *IEEE Transactions on Image Processing*, *20*(3), 681–695. 10.1109/TIP.2010.2076294, PubMed: 20840899

Bach, F., Mairal, J., Ponce, J., & Sapiro, G. (2010). Sparse coding and dictionary learning for image analysis. In *Proceedings of the IEEE International Conference on Computer Vision and Pattern Recognition*. Piscataway, NJ: IEEE.

Balavoine, A., Rozell, C. J., & Romberg, J. (2013). Convergence speed of a dynamical system for sparse recovery. *IEEE Transactions on Signal Processing*, *61*(17), 42594269. 10.1109/TSP.2013.2271482

Bian, W., & Chen, X. (2012). Smoothing neural network for constrained non-Lipschitz optimization with applications. *IEEE Transactions on Neural Networks and Learning Systems*, *23*(3), 3991411.

Boyd, S., Parikh, N., Chu, E., Peleato, B., & Eckstein, J. (2011). Distributed optimization and statistical learning via the alternating direction method of multipliers. *Foundations and Trends in Machine Learning*, *3*(1), 1–122. 10.1561/2200000016

Candès, E. J. (2008). The restricted isometry property and its implications for compressed sensing. *Comptes rendus mathematique*, *346*(9–10), 589–592.

Candès, E. J., Romberg, J. K., & Tao, T. (2006). Stable signal recovery from incomplete and inaccurate measurements. *Communications on Pure and Applied Mathematic*, *59*(8), 1207–1223.

Chartrand, R. (2007). Exact reconstruction of sparse signals via nonconvex minimization. *IEEE Signal Processing Letters*, *14*(10), 707–710. 10.1109/LSP.2007.898300

Chen, Y., Shi, L., Feng, Q., Yang, J., Shu, H., Luo, L., & Chen, W. (2014). Artifact suppressed dictionary learning for low-dose CT image processing. *IEEE Transactions on Medical Imaging*, *33*(12), 2271–2292. 10.1109/TMI.2014.2336860, PubMed: 25029378

Fan, J., & Li, R. (2001). Variable selection via nonconcave penalized likelihood and its oracle properties. *Journal of the American Statistical Association*, *96*(456), 1348–1360. 10.1198/016214501753382273

Downloaded from http://direct.mit.edu/neco/article-pdf/34/8/1727/2034959/neco_a_01508.pdf by HONG KONG POLYTECHNIC UNIVERSITY user on 13 August 2024

Feng, R., Leung, C. S., Constantinides, A. G., & Zeng, W. J. (2017). Lagrange programming neural network for non-differentiable optimization problems in sparse approximation. *IEEE Transactions on Neural Networks and Learning Systems*, *28*(10), 2395–2407. 10.1109/TNNLS.2016.2575860, PubMed: 27479978

Garg, K., & Baranwal, M. (2020). CAPPA: Continuous-time accelerated proximal point algorithm for sparse recovery. *IEEE Signal Processing Letters*, *27*, 1760–1764. 10.1109/LSP.2020.3027490

Garg, K., Baranwal, M., Gupta, R., Vasudevan, R., & Panagou, D. (2019). *Fixed-time stable proximal dynamical system for solving mixed variational inequality problems.* arXiv:1908.03517.

Garg, K., & Panagou, D. (2021). Fixed-time stable gradient flows: Applications to continuous-time optimization *IEEE Transactions on Automatic Control*, *66*(5), 2002–2015. 10.1109/TAC.2020.3001436

He, X., Wen, H., & Huang, T. (2021). A fixed-time projection neural network for solving l_1-minimization problem. *IEEE Transactions on Neural Networks and Learning Systems*, Piscataway, NJ: IEEE. 10.1109/TNNLS.2021.3088535

Huang, K., & Aviyente, S. (2006). Sparse representation for signal classification. In B. Schölkopf, J. Platt, & T. Hoffman (Eds.), *Advances in neural information processing systems*, *19* (pp. 609–616). Cambridge, MA: MIT Press.

Lai, M. J., Xu, Y., & Yin, W. (2013). Improved iteratively reweighted least squares for unconstrained smoothed l_q minimization. *SIAM Journal on Numerical Analysis*, *51*(2), 927–957. 10.1137/110840364

Li, C., Yu, X., Yu, W., Chen, G., & Wang, J. (2016). Efficient computation for sparse load shifting in demand side management. *IEEE Transactions on Smart Grid*, *8*(1), 250–261. 10.1109/TSG.2016.2521377

Li, C., Yu, X., Zhou, X., & Ren, W. (2017). A fixed time distributed optimization: A sliding mode perspective. In *Proceedings of the IECON 2017-43rd Annual Conference of the IEEE Industrial Electronics Society* (pp. 8201–8207). Piscataway, NJ: IEEE.

Li, X., Wang, J., & Kwong, S. (2020). A discrete-time neurodynamic approach to sparsity-constrained nonnegative matrix factorization. *Neural Computation*, *32*(8), 1531–1562. 10.1162/neco_a_01294, PubMed: 32521214

Li, Y., Cichocki, A., & Amari, S. I. (2006). Blind estimation of channel parameters and source components for EEG signals: A sparse factorization approach. *IEEE Transactions on Neural Networks*, *17*(2), 419–431. 10.1109/TNN.2005.863424, PubMed: 16566469

Lin, W. T., Wang, Y. W., Li, C., & Yu, X. (2020). Predefined-time optimization for distributed resource allocation. *Journal of the Franklin Institute*, *357*(16), 11323–11348. 10.1016/j.jfranklin.2019.06.024

Liu, P., Zeng, Z., & Wang, J. (2017). Multistability of delayed recurrent neural networks with Mexican hat activation functions. *Neural Computation*, *29*(2), 423–457. 10.1162/NECO_a_00922, PubMed: 28030775

Liu, Q., Cao, J., & Chen, G. (2010). A novel recurrent neural network with finite-time convergence for linear programming. *Neural Computation*, *22*(11), 2962–2978. 10.1162/NECO_a_00029, PubMed: 20804382

Liu, Q., & Wang, J. (2008). A one-layer recurrent neural network with a discontinuous activation function for linear programming. *Neural Computation*, *20*(5), 1366–1383. 10.1162/neco.2007.03-07-488

Downloaded from http://direct.mit.edu/neco/article-pdf/34/8/1727/2034959/neco_a_01508.pdf by HONG KONG POLYTECHNIC UNIVERSITY user on 13 August 2024

Liu, Q., & Wang, J. (2016). L_1-minimization algorithms for sparse signal reconstruction based on a projection neural network. *IEEE Transactions on Neural Networks and Learning Systems*, *27*(3), 698–707. 10.1109/TNNLS.2015.2481006, PubMed: 26513806

Liu, T., & Pong, T. K. (2017). Further properties of the forward-backward envelope with applications to difference-of-convex programming. *Computational Optimization and Applications*, *67*(3), 489–520. 10.1007/s10589-017-9900-2

Lou, Y., & Yan, M. (2018). Fast L_1-L_2 minimization via a proximal operator. *Journal of Scientific Computing*, *74*(2), 767–785. 10.1007/s10915-017-0463-2

Lou, Y., Yin, P., & Xin, J. (2016). Point source super-resolution via non-convex l_1 based methods. *Journal of Scientific Computing*, *68*(3), 1082–1100. 10.1007/s10915-016-0169-x

Polyakov, A. (2012). Nonlinear feedback design for fixed-time stabilization of linear control systems. *IEEE Transactions on Automatic Control*, *57*(8), 2106–2110. 10.1109/TAC.2011.2179869

Qin, J., & Lou, Y. (2019). L_{1-2} regularized logistic regression. In *Proceedings of the 2019 53rd Asilomar Conference on Signals, Systems, and Computers* (pp. 779–783). Piscataway, NJ: IEEE.

Ren, J., Yu, L., Lyu, C., Zheng, G., Barbot, J. P., & Sun, H. (2019). Dynamical sparse signal recovery with fixed-time convergence. *Signal Processing*, *162*, 65–74. 10.1016/j.sigpro.2019.04.010

Rozell, C. J., Johnson, D. H., Baraniuk, R. G., & Olshausen, B. A. (2008). Sparse coding via thresholding and local competition in neural circuits. *Neural Computation*, *20*, 2526–2563. 10.1162/neco.2008.03-07-486, PubMed: 18439138

Tomioka, R., & Sugiyama, M. (2009). Dual-augmented Lagrangian method for efficient sparse reconstruction. *IEEE Signal Processing Letters*, *16*(12), 1067–1070. 10.1109/LSP.2009.2030111

Wagner, A., Wright, J., Ganesh, A., Zhou, Z., Mobahi, H., & Ma, Y. (2011). Toward a practical face recognition system: Robust alignment and illumination by sparse representation. *IEEE Transactions on Pattern Analysis and Machine Intelligence*, *34*(2), 372–386. 10.1109/TPAMI.2011.112

Wang, D., & Zhang, Z. (2017). Generalized sparse recovery model and its neural dynamical optimization method for compressed sensing. *Circuits, Systems, and Signal Processing*, *36*(11), 4326–4353. 10.1007/s00034-017-0532-7

Wen, H., Wang, H., & He, X. (2020). A neurodynamic algorithm for sparse signal reconstruction with finite-time convergence. *Circuits, Systems, and Signal Processing*, *39*, 6058–6072. 10.1007/s00034-020-01445-3

Wright, J., Ma, Y., Mairal, J., Sapiro, G., Huang, T. S., & Yan, S. (2010). Sparse representation for computer vision and pattern recognition. In *Proceedings of the IEEE*, *98*, 1031–1044. 10.1109/JPROC.2010.2044470

Wu, L., Sun, Z., & Li, D. H. (2016). A Barzilai-Borwein-like iterative half thresholding algorithm for the $l_{1/2}$ regularized problem. *Journal of Scientific Computing*, *67*(3), 581–601. 10.1007/s10915-015-0094-4

Xu, B., Liu, Q., & Huang, T. (2019). A discrete-time projection neural network for sparse signal reconstruction with application to face recognition. *IEEE Transactions on Neural Networks and Learning Systems*, *30*(1), 151–162. 10.1109/TNNLS.2018.2836933, PubMed: 29994338

Downloaded from http://direct.mit.edu/neco/article-pdf/34/8/1727/2034959/neco_a_01508.pdf by HONG KONG POLYTECHNIC UNIVERSITY user on 13 August 2024

Xu, Z., Chang, X., Xu, F., & Zhang, H. (2012). $L_{1/2}$ regularization: A thresholding representation theory and a fast solver. *IEEE Transactions on Neural Networks and Learning Systems*, *23*(7), 1013–1027. 10.1109/TNNLS.2012.2197412, PubMed: 24807129

Yin, P., Lou, Y., He, Q., & Xin, J. (2015). Minimization of l_1-l_2 for compressed sensing. *SIAM Journal on Scientific Computing*, *37*(1), A536–A563. 10.1137/140952363

Yu, L., Zheng, G., & Barbot, J. P. (2017). Dynamical sparse recovery with finite-time convergence. *IEEE Transactions on Signal Processing*, *65*(23), 6146–6157. 10.1109/TSP.2017.2745468

Zhang, S., & Xin, J. (2018). Minimization of transformed l_1 penalty: Theory, difference of convex function algorithm, and robust application in compressed sensing. *Mathematical Programming*, *169*(1), 307–336. 10.1007/s10107-018-1236-x

Zhao, Y., He, X., Huang, T., & Huang, J. (2018). Smoothing inertial projection neural network for minimization l_{p-q} in sparse signal reconstruction. *Neural Networks*, *99*, 31–41. 10.1016/j.neunet.2017.12.008, PubMed: 29306802

Zhao, Y., Liao, X., He, X., Tang, R., & Deng, W. (2021). Smoothing inertial neurodynamic approach for sparse signal reconstruction via l_p-norm minimization. *Neural Networks*, *140*, 100–112. 10.1016/j.neunet.2021.02.006, PubMed: 33752140

Zhu, L., Wang, J., He, X., & Zhao, Y. (2018). An inertial projection neural network for sparse signal reconstruction via l_{1-2} minimization. *Neurocomputing*, *315*, 89–95. 10.1016/j.neucom.2018.06.050

Zuo, W., Meng, D., Zhang, L., Feng, X., & Zhang, D. (2013). A generalized iterated shrinkage algorithm for non-convex sparse coding. In *Proceedings of the IEEE International Conference on Computer Vision* (pp. 217–224). Piscataway, NJ: IEEE.

Received October 8, 2021; accepted February 27, 2022.

Downloaded from http://direct.mit.edu/neco/article-pdf/34/8/1727/2034959/neco_a_01508.pdf by HONG KONG POLYTECHNIC UNIVERSITY user on 13 August 2024